Circular RNA circ-ACACA regulates proliferation, migration and glycolysis in non-small-cell lung carcinoma via miR-1183 and PI3K/PKB pathway

WENWEN WU, WEI XI, HUIMIN LI, MENGXIANG YANG and XIALEI YAO

Department of Oncology, Liaocheng People's Hospital, Liaocheng, Shandong 252000, P.R. China

Received October 25, 2019; Accepted January 24, 2020

DOI: 10.3892/ijmm.2020.4549

Abstract. Non-small cell lung carcinoma (NSCLC) accounts for 85% of all lung cancers and the five-year survival rate is ~1% in the late stage. Circular RNAs (circRNAs) were reported to be involved in the progression of diverse human cancers. However, the role of circ-ACACA in NSCLC progression remains elusive. Quantitative polymerase chain reaction was conducted to detect the expression levels of circ-ACACA and microRNA (miR)-1183 in NSCLC tissues and cells. A Cell Counting Kit-8 assay and transwell assay were employed to check proliferation and migration, respectively. Metabolic alternations in NSCLC cells were monitored by the Seahorse XFe96 analyzer. The protein levels of cellular myelocytomatosis, matrix metallopeptidase 9, glucose transporter 1, phosphatase and tensin homolog, phosphoinositide 3-kinases (PI3K), phosphorylated PI3K (p-PI3K), protein kinase B (PKB) and p-PKB in samples were measured by western blotting. The interaction between circ-ACACA and miR-1183 was predicted by circular RNA Interactome, which was verified by dual-luciferase reporter assay, RNA immunoprecipitation assay and RNA pull-down assay. Xenograft tumor model was established to investigate the biological roles of circ-ACACA *in vivo*. The level of circ-ACACA was markedly upregulated in NSCLC tissues and cells, which was contrary to the expression of miR-1183. Knockdown of circ-ACACA inhibited proliferation and migration of NSCLC cells and also reduced the glycolysis rate. In addition, miR-1183 was a target of circ-ACACA and its downregulation reversed circ-ACACA silencing-mediated inhibitory impact on NSCLC progression. Further studies indicated that circ-ACACA regulated the PI3K/PKB pathway through interacting with miR-1183 and downregulation of circ-ACACA suppressed tumor growth. Knockdown of circ-ACACA impeded NSCLC progression by sponging miR-1183 and inactivating the PI3K/PKB signaling pathway.

Correspondence to: Mr. Xialei Yao, Department of Oncology, Liaocheng People's Hospital, 67 Dongchang West Road, Liaocheng, Shandong 252000, P.R. China
E-mail: cehaom@163.com

Key words: non-small cell lung carcinoma, circular-ACACA, miR-1183, phosphoinositide 3-kinase/protein kinase B pathway

Introduction

Non-small cell lung carcinoma (NSCLC) is a growing threat to humans and the dominant cause of cancer-related deaths worldwide (1). The five-year overall survival is not optimistic due to metastasis and chemoresistance (2,3). Hence, it is pressing to find novel molecular targets for NSCLC treatment.

Circular RNAs (circRNAs), a type of single-stranded RNAs which form a covalently closed continuous loop, are produced by backsplicing (4) and they are resistant to exonuclease-mediated degradation (5). Growing evidence has proved that circRNAs are associated with colon cancer (6), gastric cancer (7), bladder cancer (8) and NSCLC (9,10). Microarray data showed that hsa_circ_0106705 (circ-ACACA) was upregulated in human lung cancer according to Yang *et al* (11). However, the regulatory mechanism of circ-ACACA in NSCLC is hardly reported and needs to be investigated further.

MicroRNAs (miRNAs/miRs) are short (~22 nucleotides) and highly conserved noncoding RNAs, which mediate gene expression by binding to the 3'-untranslated region of mRNA at the post-transcriptional level (12). Numerous studies have emphasized the core position of miRNAs in governing cancer development (13,14). miR-1183 was reported to be dysregulated in numerous human diseases (15-17) and Zhou *et al* (18) reported that miR-1183 functioned in the tumorigenesis of NSCLC. Nevertheless, the precise mechanism of miR-1183 in NSCLC progression remains to be studied.

The phosphoinositide 3-kinases/protein kinase B (PI3K/PKB) pathway is essential for cell survival and apoptosis (19) and their aberrant activation is usually correlated with malignancy (20). A previous study indicated that the PI3K/PKB pathway was associated with the initiation of endometrial cancer (21) and cisplatin-resistance in NSCLC (22). Therefore, in-depth studies of the PI3K/PKB signaling pathway could contribute to the development of new effective therapeutic methods for NSCLC.

In this study, the expression level of circ-ACACA in NSCLC tissues and cells was first measured. Afterwards, the function and potential regulatory mechanism of circ-ACACA in NSCLC were further investigated by subsequent experiments.

Materials and methods

Specimens and cell culture. A total of 60 NSCLC tissues and paired nearby healthy tissues were sourced from patients with NSCLC (36 males and 24 females; 20-65 years old) who had undergone surgical resection between April 2015 to August 2017 at Liaocheng People's Hospital, and the 60 NSCLC tissues included 37 early stages (I and II) tissues and 23 advanced stages (III and IV) tissues or contained 21 lymphoid node metastasis tissues and 39 controls. Tumor, node and metastasis (TNM) staging was classified according to the 7th edition of the American Joint Committee on Cancer TNM classification based on information obtained regarding the tumor during tumor surgery and histological or imaging studies. Every patient signed the informed consent and the official approval from the Ethics Committee of Liaocheng People's Hospital was obtained in this study. Human normal bronchus epithelium cell line (BEAS-2B) and NSCLC cell lines (A549, H1975, H1395, H1793, H1299 and H1792) were purchased from the American Type Culture Collection. McCoy's 5A medium (Sigma-Aldrich; Merck KGaA), containing 5% CO_2 and 10% fetal bovine serum (FBS; Sigma-Aldrich; Merck KGaA) was used to culture cells.

Cell transfection. Small interfering (si) RNA against circ-ACACA (si-circ-ACACA; 5'-GAAAGACUUUGAAAU ACUCGU-3'), negative control of siRNA (si-NC; 5'-AAG ACAUUGUGUGUCCGCCTT-3'), miR-1183 mimic (named as miR-1183; 5'-CACUGUAGGUGAUGGUGAGAGUGG GCA-3') and mimic negative control (miR-NC; 5'-ACG UGACACGUUCGGAGAATT-3'), and miR-1183 inhibitor (anti-miR-1183; 5'-UGCCCACUCUCACCAUCACCUACA GUG-3') and corresponding negative control (anti-NC; 5'-UGA GCUGCAUAGAGUAGUGAUUA-3') were obtained from Shanghai GenePharma Co., Ltd. A549 and H1299 cells were transfected with the above oligonucleotides (at a final concentration of 50 nM) using Lipofectamine 2000 Transfection Reagent (Beijing Solarbio Science & Technology Co., Ltd.) for 24 h referring to the manufacturer's protocol.

RNA isolation, reverse transcription-quantitative polymerase chain reaction (RT-qPCR) and RNase R treatment. NSCLC tissues and cells were collected and total RNA was isolated by the TriQuick Reagent (Beijing Solarbio Science & Technology Co., Ltd.). Then, RNA was reverse transcribed to cDNA (37˚C for 15 min; 85˚C for 5 sec; hold at 4˚C) by PrimeScript™ RT Master Mix kit (Takara Biotechnology, Co., Ltd.). qPCR was conducted (95˚C for 5 min, then 40 cycles of 95˚C for 15 sec, 60˚C for 30 sec and 72˚C for 45 sec) with SYBR Green Realtime PCR Master Mix (Beijing Solarbio Science & Technology Co., Ltd.) and data were analyzed using $2^{-\Delta\Delta Cq}$ method (23). β-actin and U6 were introduced as the inner references. Primers in the present research: circ-ACACA (forward 5'-GTGGCTTTG AAGGAGCTGTC-3', reverse 5'-CAGACATGCTGGACC TTGAA-3'); miR-1183 (forward, 5'-ACTGACCACTGTAGG TGATGGT-3', reverse 5'-GCGAGCACAGAATTAATACGA CTCACTATAGG-3'); β-actin (forward 5'-GCACCACAC CTTCTACAATG-3', reverse, 5'-TGCTTGCTGATCCACAT CTG-3'); U6 (forward, 5'-TCCGGGTGATGCTTTTCCTAG-3' and reverse, 5'-CGCTTCACGAATTTGCGTGTCAT-3'). Purified RNAs were treated with RNase R (Beijing Solarbio Science & Technology Co., Ltd.) for subsequent experiments.

Cell Counting Kit-8 (CCK-8) assay. Cell proliferation was tested with CCK-8 reagent (Beyotime Institute of Biotechnology) according to the manufacturer's protocol. After transfection, A549 and H1299 cells were seeded into 96-well plates and then incubated with 10 μl CCK-8 solution for 2 h. Optical density values were examined at 450 nm wavelength using a microplate reader (Bio-Rad Laboratories, Inc.).

Transwell assay. A Transwell chamber was employed to check the capacity of cell migration. Transfected cells ($5x10^4$ cells) were seeded into the upper chamber and medium containing FBS was placed in the lower chamber. After being treated with 0.1% crystal violet for 20 min at room temperature (Beijing Solarbio Science & Technology Co., Ltd.) following incubation for 24 h, migrated cells were analyzed under an inverted light microscope (MTX Lab Systems).

Glycolysis analysis. Glycolysis was evaluated by using Seahorse XF glycolytic rate assay kit (Agilent Technologies, Inc.) on Seahorse XFe96 analyzer (Agilent Technologies, Inc.). Cells ($2x10^4$ cells/well) transfected with si-circ-ACACA, anti-miR-1183, si-circ-ACACA + anti-miR-1183 or their matched controls were seeded in the XF96 well plate. After the probes were calibrated, 10 mmol glucose, 10 μmol oligomycin and 50 mmol 2-deoxyglucose were serially injected to measure the extracellular acidification rate (ECAR). Data were analyzed with Seahorse XFe24 Wave software version Wave 2.2 (Agilent Technologies, Inc.).

Western blotting. Proteins from samples were isolated using RIPA buffer (Vazyme) and protein concentration was checked by Detergent Compatible Bradford Protein Quantification kit (Vazyme). Proteins (20 μg/lane) were separated by 10% SDS-PAGE and then transferred onto the polyvinylidene difluoride membranes (Vazyme). The membranes were blocked with 5% skimmed milk (Vazyme) for 1 h at room temperature and washed by phosphate-buffered saline. Afterwards, the membranes were incubated at 4˚C overnight with the primary antibodies: Cellular-myelocytomatosis (c-myc; 1:1,000; cat. no. ab32072; Abcam), matrix metallopeptidase 9 (MMP9; 1:1,000; cat. no. ab38898; Abcam), glucose transporter 1 (GLUT-1; 1:1,000; cat. no. ab652; Abcam), phosphatase and tensin homolog (PTEN; 1:3,000; cat. no. ab32199; Abcam), phosphoinositide 3-kinases (PI3K; 1:2,000; cat. no. ab151549; Abcam), phosphorylated PI3K (p-PI3K; 1:1,000; cat. no. ab138364; Abcam), PKB (1:1,000; cat. no. ab8805; Abcam), phosphorylated PKB (p-PKB; 1:1,000; cat. no. ab38449; Abcam) or β-actin (1:3,000; cat. no. ab8227; Abcam) overnight. After being rewashed, the membranes were incubated with the horseradish peroxidase-conjugated goat anti-rabbit secondary antibody (1:3,000; cat. no. ab205718; Abcam) for 3 h at 37˚C. The membranes were analyzed by the ChemiDoc™ MP Imaging System with Image Lab™ Software version5.2 (Bio-Rad Laboratories, Inc.) after being treated with an Enhanced ECL Chemiluminescence Detection kit (Vazyme).

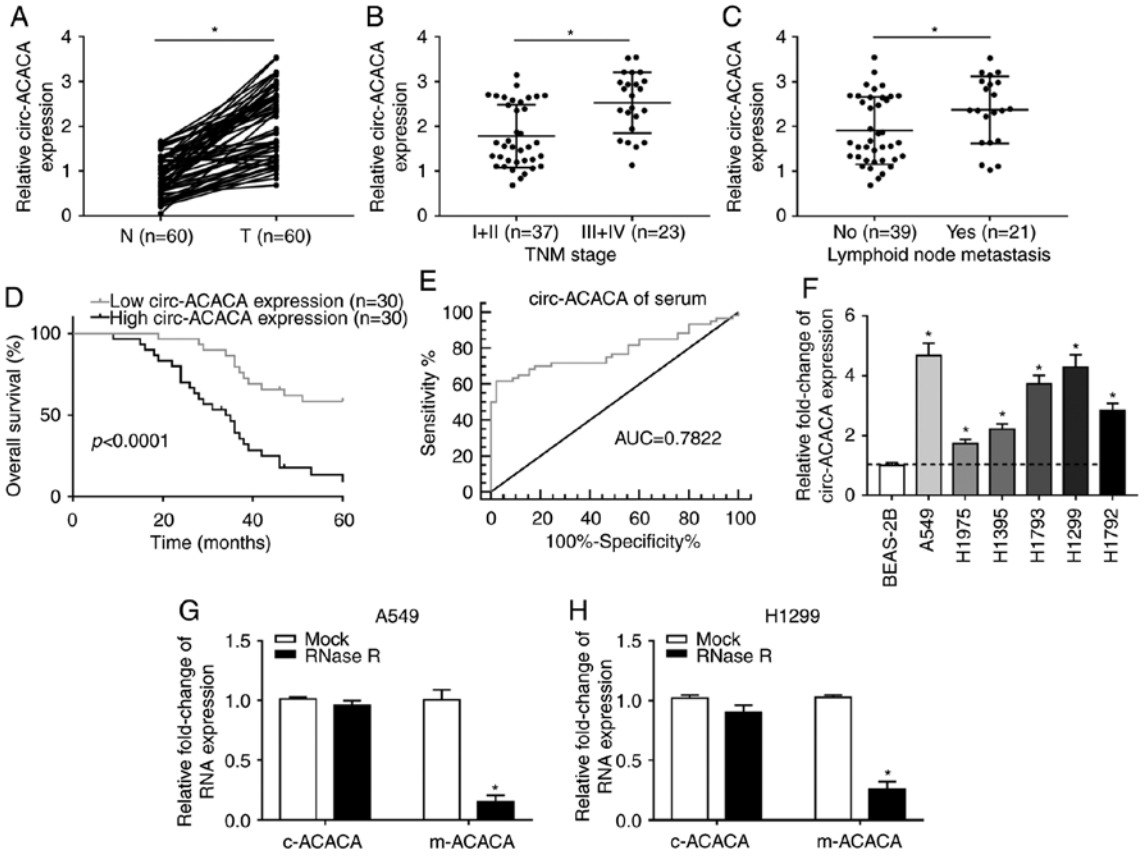

Figure 1. circ-ACACA functions as an oncogene in NSCLC. (A) The expression level of circ-ACACA was detected by RT-qPCR in NSCLC tissues (n=60) and normal tissues (n=60). (B) The level of circ-ACACA in different tumor, node and metastasis stages was checked by RT-qPCR. (C) The level of circ-ACACA in lymphoid node metastatic tissues or not was checked by RT-qPCR. (D) The Kaplan-Meier method was utilized to estimate overall survival and the log-rank test was used to evaluate the differences between survival curves. (E) Receiver operating characteristic curve analysis was used to evaluate the diagnostic value of circ-ACACA in NSCLC. (F) The level of circ-ACACA in the normal cell line and NSCLC cell lines was measured by RT-qPCR. The relative expression of c-ACACA and m-ACACA in NSCLC (G) A549 and (H) H1299 cells treated with RNase R or not was measured by RT-qPCR. *P<0.05 vs. BEAS-2B or mock. RT-q, reverse transcription-quantitative; circ, circular; NSCLC, non-small cell lung cancer; TNM, tumor node metastasis; AUC, area under the curve; c-ACACA, mRNA of circ-ACACA; m-ACACA, mRNA of ACACA.

Dual-luciferase reporter assay. The potential complementary sequences of circ-ACACA and miR -1183 were forecasted by circular RNA Interactome (24). The wild type (WT) sequence of circ-ACACA harboring the binding sites of miR-1183 was inserted into the pGL3 vector (Promega Corporation) to establish the luciferase reporter vector WT-circ-ACACA. Similarly, the mutant (MUT)-circ-ACACA reporter vector was established by mutating the potential target sites of miR-1183. Then, the luciferase reporter vectors (100 ng) were cotransfected with 50 ng miR-1183 or miR-NC into A549 and H1299 cells for 24 h using Lipofectamine 2000 (Beijing Solarbio Science & Technology, Co., Ltd.). Firefly luciferase activities were normalized by comparison with *Renilla* luciferase. The Dual-Glo Luciferase Assay System kit (Promega Corporation) was utilized to measure luciferase activity.

RNA immunoprecipitation (RIP) assay. RIP was carried out using Magna RIP RNA-Binding Protein Immunoprecipitation kit (EMD Millipore) following the manufacturer's protocols. Briefly, harvested cells were lysed with RIPA lysis buffer (Beyotime Institute of Biotechnology) and incubated with magnetic beads conjugated with anti-Argonaute 2 (Anti-Ago2) antibody (1:5,000; cat. no. MABE253; EMD Millipore) for 8 h at 37˚C, and immunoglobulin G (IgG; 1:5,000; cat. no. 12-370; EMD Millipore) was used as a negative control. The protein was removed by Proteinase K. The immune precipitated RNA was purified and analyzed by RT-qPCR.

RNA pull-down assay. A biotin-labeled probe against miR-1183 (named as Bio-miR-1183) and its negative control (named as Bio-NC) were obtained from Sangon Biotech Co., Ltd. Transfected cells were lysed with RIPA lysis buffer (Beyotime Institute of Biotechnology) and incubated with streptavidin-coupled beads (Sangon Biotech Co., Ltd.). After being treated by proteinase K, circ-ACACA was isolated and checked by RT-qPCR.

Xenograft mice model. BALB/c nude mice (male; 5 weeks old; ~18-23 g; n=10) were acquired from Shanghai LingChang Biotech Co., Ltd. (Shanghai SLAC Laboratory Animal Co., Ltd.) and kept in specific pathogen free conditions (temperature 23±2˚C, relative humidity 55±5%, 12 h/12 h light/dark cycle with *ad libitum* access to water and food). The mice were randomly grouped into two groups (n=5 each). Lentivirus harboring short hairpin RNA targeting circ-ACACA (named as sh-circ-ACACA) and negative control (sh-NC) were constructed by GeneCopoeia, Inc. A549 cells at a density of $1x10^6$ cells/well in 6-well culture plates were infected with 4 μg of filtered

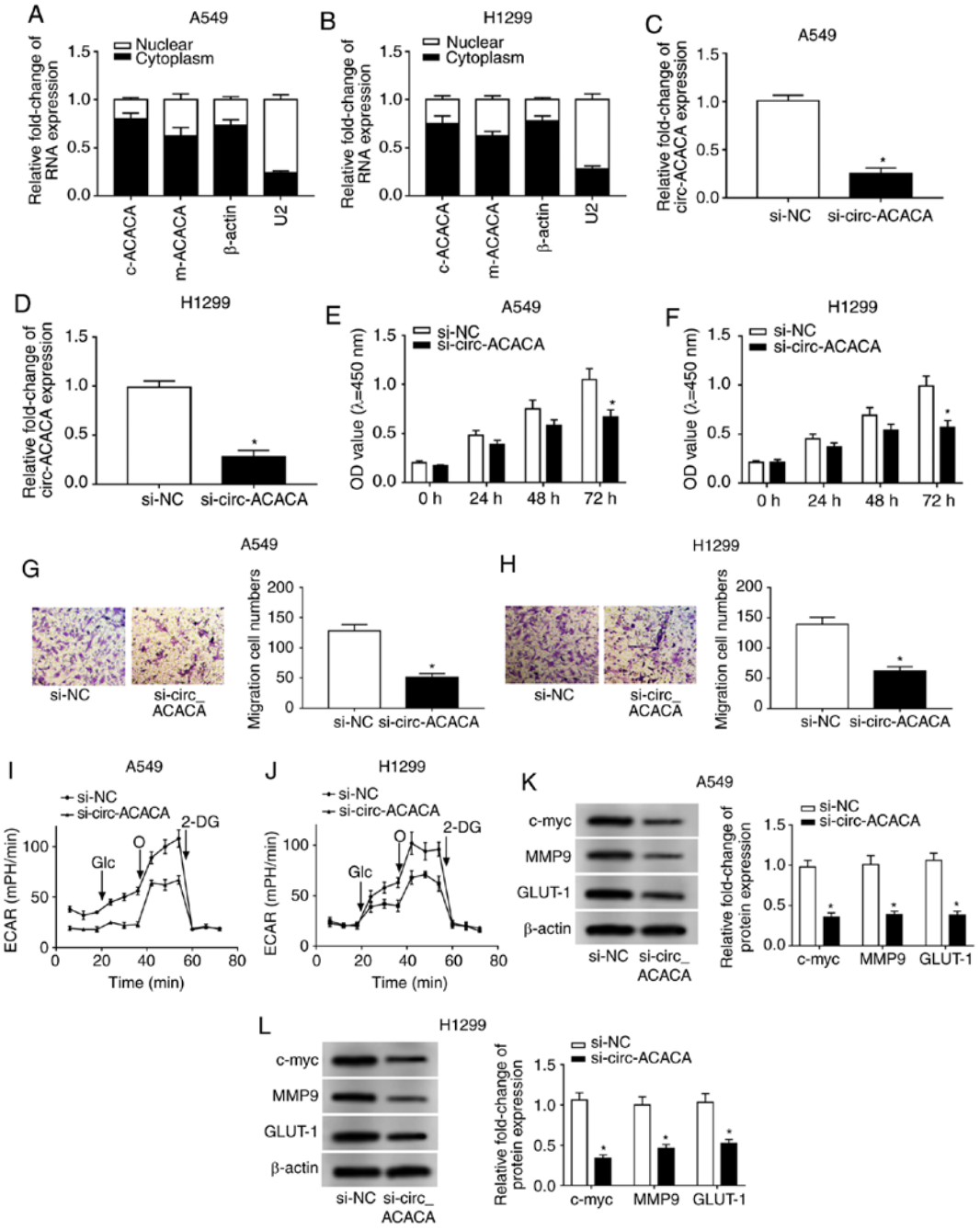

Figure 2. circ-ACACA silencing hampers the progression of NSCLC. The levels of c-ACACA and m-ACACA in nucleus and cytoplasm were detected by RT-qPCR of (A) A549 and (B) H1299 cells. β-actin and U2 were applied as positive controls in the cytoplasm and nucleus, respectively. The level of circ-ACACA in NSCLC cells infected with si-circ-ACACA or si-NC was checked by RT-qPCR in (C) A549 and (D) H1299 cells. Cell Counting Kit-8 assay was used to check proliferation of infected (E) A549 and (F) H1299 cells. A Transwell assay was performed to evaluate the ability of migration of infected (G) A549 and (H) H1299 cells. The glycolysis rate was detected by Seahorse XFe96 analyzer in (I) A549 and (J) H1299 cells. The protein levels of c-myc, MMP9 and GLUT-1 in infected (K) A549 and (L) H1299 cells were checked by western blotting. *P<0.05 vs. si-NC. RT-q, reverse transcription-quantitative; circ, circular; NSCLC, non-small cell lung cancer; si, small interfering; NC, negative control; MMP, matrix metalloproteinases; GLUT, glucose transporter; c-myc, cellular-myelocytomatosis; OD, optical density; ECAR, extracellular acidification rate; Glc, glucose; O, oligomycin; 2-DG, 2-deoxyglucose.

lentivirus plus 8 μg/ml polybrene (Sigma-Aldrich; Merck KGaA) for 48 h and subsequently selected by 2.5 μg/ml puromycin (Invitrogen; Thermo Fisher Scientific, Inc.) for at least 3 days to establish stable cell lines. A total of ~2x10^6 A549 cells infected with sh-circ-ACACA or sh-NC plasmid DNA in 200 μl of FBS-free culture medium were injected subcutaneously into the flank of the nude mice. The tumor volume was calculated every 7 days according to the formula: 0.5 x length x width^2. The tumor weight was measured after the mice were euthanized. The mRNA or protein levels of corresponding genes in tumors were checked by RT-qPCR or western blotting, respectively. The animal experiment was approved by the Animal Care and Use Committee of Liaocheng People's Hospital and executed referring to the instructions of the National Animal Protection and Ethics Institute.

Statistical analysis. Experimental data were calculated by GraphPad Prism 8.0 (GraphPad Software, Inc.) and presented

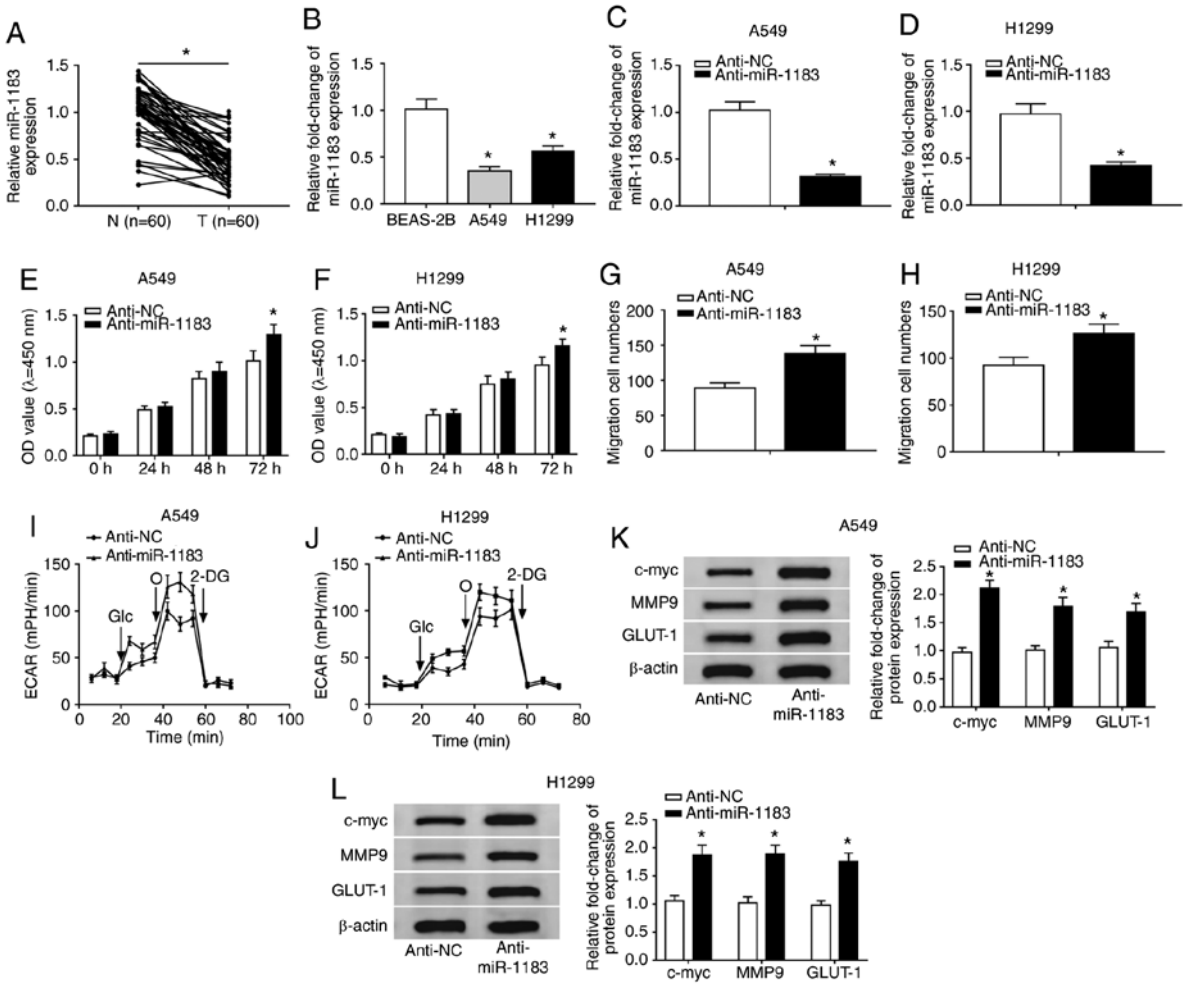

Figure 3. miR-1183 inhibitor promotes the progression of NSCLC. (A) The expression level of miR-1183 in NSCLC tissues (n=60) and normal tissues (n=60) was detected by RT-qPCR. (B) The level of miR-1183 in normal cell line and NSCLC cell lines was detected by RT-qPCR. The level of miR-1183 in (C) A549 and (D) H1299 cells infected with anti-miR-1183 or anti-NC was checked by RT-qPCR. The Cell Counting Kit-8 assay was used to check proliferation of infected (E) A549 and (F) H1299 cells. Transwell assay was utilized to check the ability of migration of infected in (G) A549 and (H) H1299 cells. The glycolysis rate was detected by Seahorse XFe96 analyzer in (I) A549 and (J) H1299 cells. The protein levels of c-myc, MMP9 and GLUT-1 in infected NSCLC cells were measured by western blotting in (K) A549 and (L) H1299 cells. *P<0.05 vs. BEAS-2B or anti-NC. RT-q, reverse transcription-quantitative; circ, circular; NSCLC, non-small cell lung cancer; si, small interfering; NC, negative control; MMP, matrix metalloproteinases; GLUT, glucose transporter; c-myc, cellular-myelocytomatosis; OD, optical density; ECAR, extracellular acidification rate; miR, microRNA; Glc, glucose; O, oligomycin; 2-DG, 2-deoxyglucose.

as the mean ± standard deviation. Two independent groups were compared by using Student's t-test. For more than two groups, the one-way analysis of variance followed by Tukey post hoc test was utilized to assess the difference. Receiver operating characteristic (ROC) curve analysis was performed referring to a previous study (25). The Kaplan-Meier method was utilized to assess overall survival and the log-rank test was used to analyze the differences between survival curves. Pearson's correlation coefficient was applied to analyze the correlation between circ-ACACA and miR-1183 in NSCLC tissues. Every experiment was repeated at least three times independently. P<0.05 was considered to indicate a statistically significant difference.

Results

circ-ACACA is significantly upregulated in NSCLC and correlates with the poor prognosis. To explore the role of circ-ACACA in NSCLC, the expression patterns were first checked. The RT-qPCR data showed that circ-ACACA was significantly upregulated in NSCLC tissues compared with paired normal tissues (Fig. 1A). Next, the correlation between circ-ACACA expression and NSCLC progression was evaluated and the results showed that the level of circ-ACACA was increased in advanced stages (III and IV) compared with early stages (I and II; Fig. 1B). In addition, metastatic samples displayed an upregulated level of circ-ACACA (Fig. 1C) and the higher level of circ-ACACA led to the lower survival rate (Fig. 1D). Also, the diagnostic accuracy of circ-ACACA was assessed using the ROC curve analysis and the data showed that the area under the ROC curve was 0.7822 (Fig. 1E), which indicated that circ-ACACA might be a hallmark of NSCLC. Moreover, circ-ACACA was also significantly upregulated in NSCLC cells (Fig. 1F). Further analysis indicated that the mRNA of circ-ACACA (c-ACACA) was conspicuously resistant to RNase R compared with the mRNA of ACACA (m-ACACA; Fig. 1G and H). Collectively, these results illuminated that circ-ACACA might act an oncogene in NSCLC and have clinical diagnostic value.

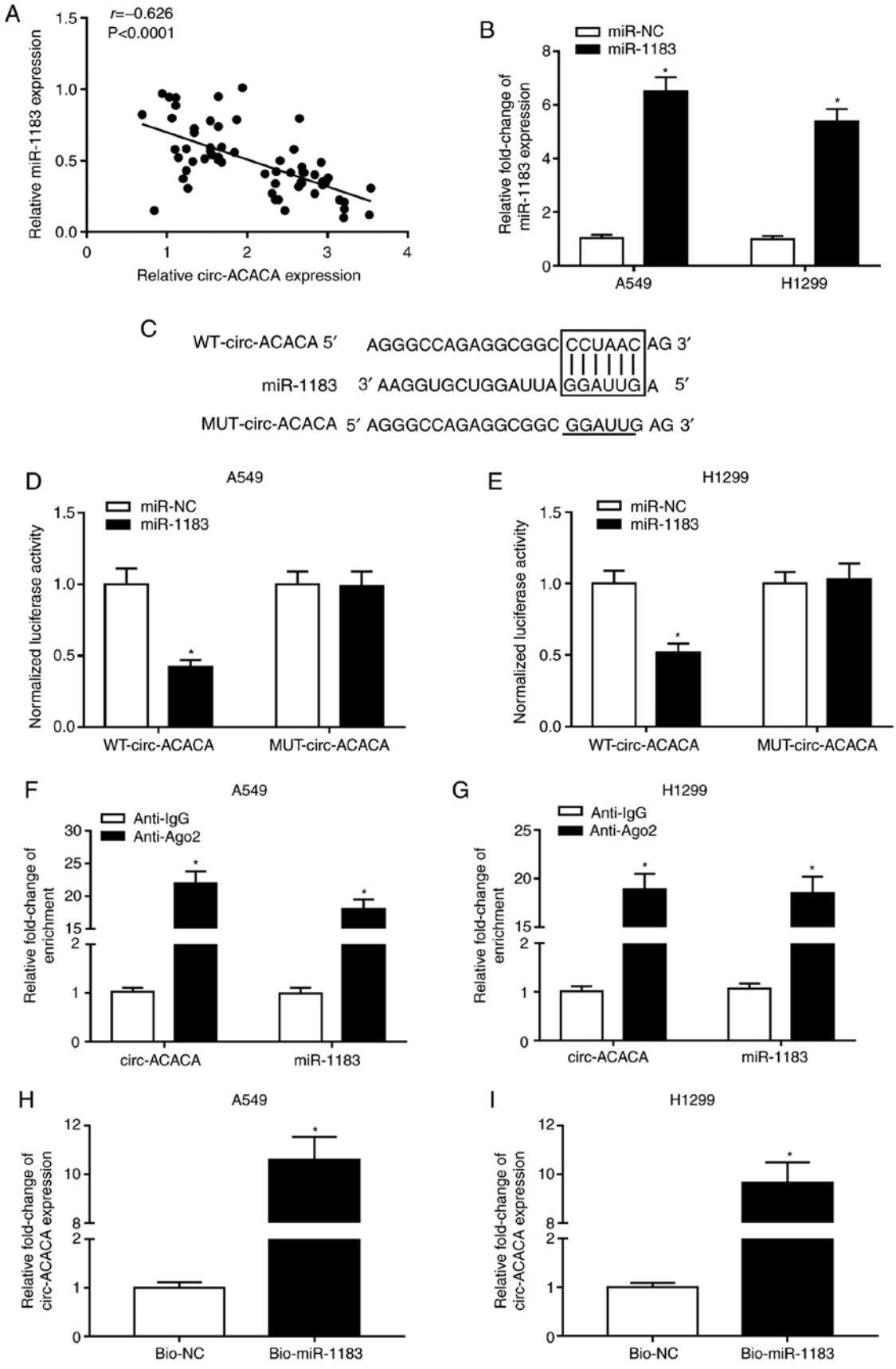

Figure 4. miR-1183 is a target of circ-ACACA and is negatively regulated by circ-ACACA in NSCLC. (A) The correlation between circ-ACACA and miR-1183 in NSCLC tissues was analyzed using Pearson's correlation coefficient. (B) The level of miR-1183 in NSCLC cells transfected with miR-1183 or miR-NC was determined by RT-qPCR. (C) The putative binding sites between circ-ACACA and miR-1183 were predicted by circular RNA Interactome. The dual-luciferase reporter assay was used to check the luciferase activity of (D) A549 and (E) H1299 cells cotransfected with the miR-1183 and WT-circ-ACACA or MUT-circ-ACACA. The RIP assay was conducted in (F) A549 and (G) H1299 cells using Anti-Ago2 to investigate the relationship between circ-ACACA and miR-1183 and Anti-IgG was used as the control. RNA pull-down was performed in (H) A549 and (I) H1299 cells and the relative enrichment of circ-ACACA in samples was detected by RT-qPCR.

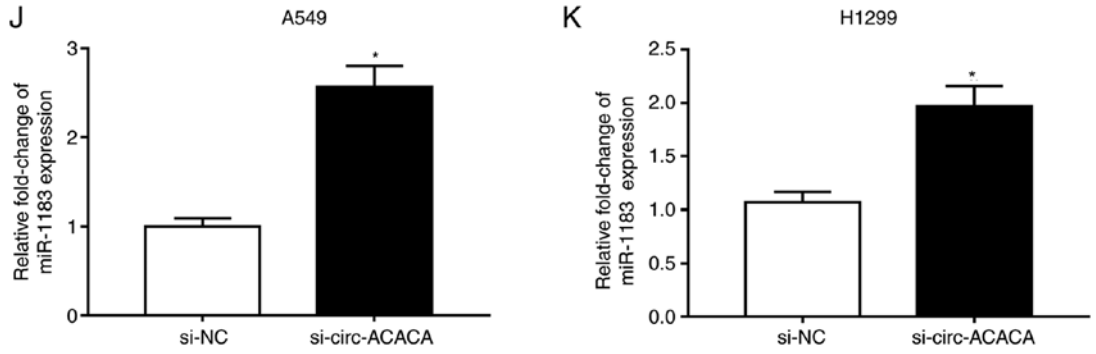

Figure 4. Continued. miR-1183 is a target of circ-ACACA and is negatively regulated by circ-ACACA in NSCLC. The level of miR-1183 in (J) A549 and (K) H1299 cells transfected with si-circ-ACACA and si-NC was measured by RT-qPCR. *P<0.05 vs. miR-NC, Anti-IgG, Bio-NC or si-NC. RT-q, reverse transcription-quantitative; circ, circular; NSCLC, non-small cell lung cancer; si, small interfering; NC, negative control; WT, wild-type; MUT, mutant; miR, microRNA; RIP, RNA immunoprecipitation; IgG, immunoglobulin.

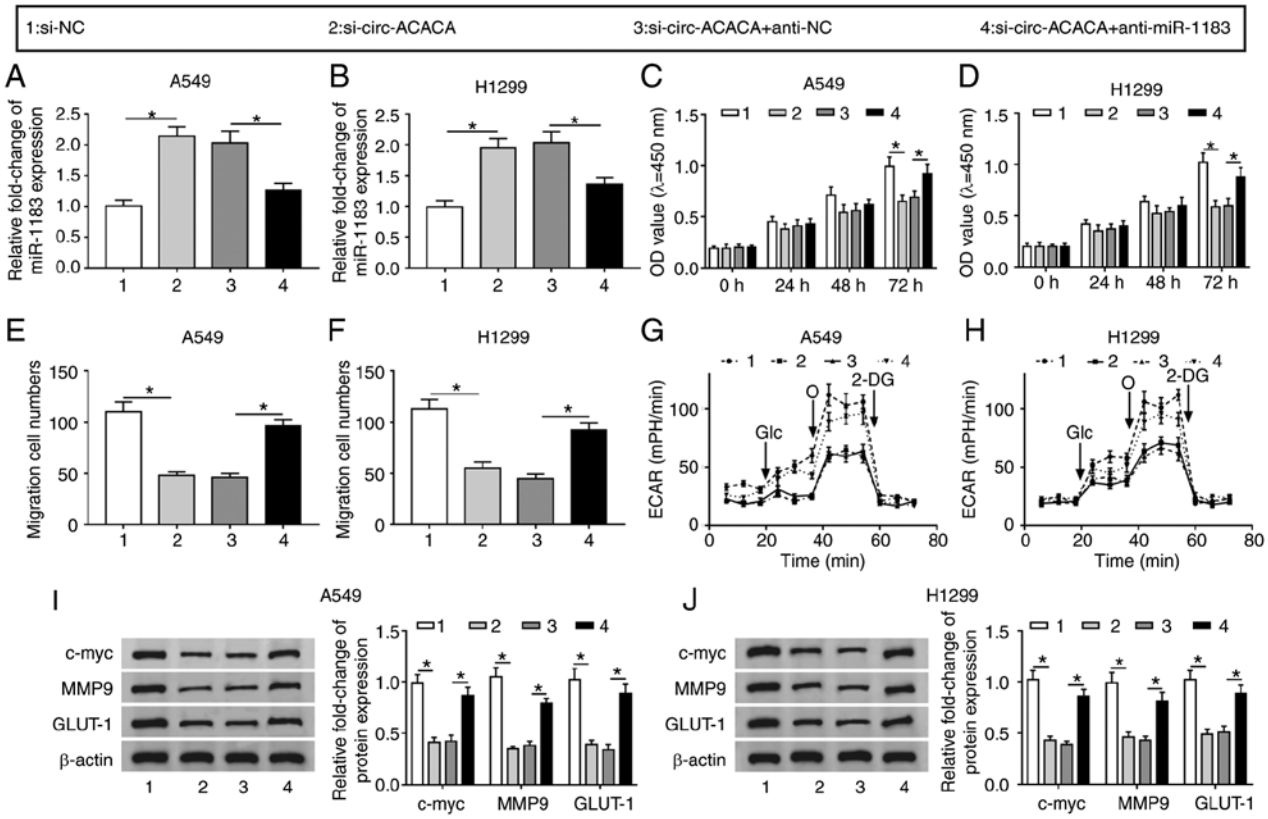

Figure 5. circ-ACACA/miR-1183 axis regulates the progression of NSCLC. The level of miR-1183 in (A) A549 and (B) H1299 cells infected with si-circ-ACACA or si-circ-ACACA + anti-miR-1183, as well as matched controls was checked by reverse transcription-quantitative PCR. Cell Counting Kit-8 assay was employed to measure proliferation of infected in (C) A549 and (D) H1299 cells. The ability of migration of infected (E) A549 and (F) H1299 cells was evaluated by Transwell assay. The glycolysis rate was detected by Seahorse XFe96 analyzer in (G) A549 and (H) H1299 cells. The protein levels of c-myc, MMP9 and GLUT-1 in infected (I) A549 and (J) H1299 cells were checked by western blotting. *P<0.05. circ, circular; NSCLC, non-small cell lung cancer; si, small interfering; NC, negative control; MMP, matrix metalloproteinases; GLUT, glucose transporter; c-myc, cellular-myelocytomatosis; OD, optical density; ECAR, extracellular acidification rate; miR, microRNA; Glc, glucose; O, oligomycin; 2-DG, 2-deoxyglucose.

Knockdown of circ-ACACA inhibits proliferation and migration and retards glycolysis rate. The levels of c-ACACA and m-ACACA were checked and the data showed that they were abundant in the cytoplasm of NSCLC cells (Fig. 2A and B). To investigate the function of circ-ACACA in NSCLC, A549 and H1299 cells were first infected with si-circ-ACACA or si-NC and then the knockdown efficiency was confirmed (Fig. 2C and D). The CCK-8 assay showed that downregulation of circ-ACACA inhibited proliferation of NSCLC cells (Fig. 2E and F) and the transwell assay indicated that knockdown of circ-ACACA weakened the ability of migration of NSCLC cells (Fig. 2G and H). Glycolysis analysis indicated that circ-ACACA silencing decreased ECAR in NSCLC cells (Fig. 2I and J). Afterwards, the protein levels of c-myc (related to proliferation), MMP9 (related to migration) and GLUT-1 (related to glycolysis) were measured and the results indicated that downregulation of circ-ACACA significantly reduced the expression of these proteins in NSCLC cells (Fig. 2K and L).

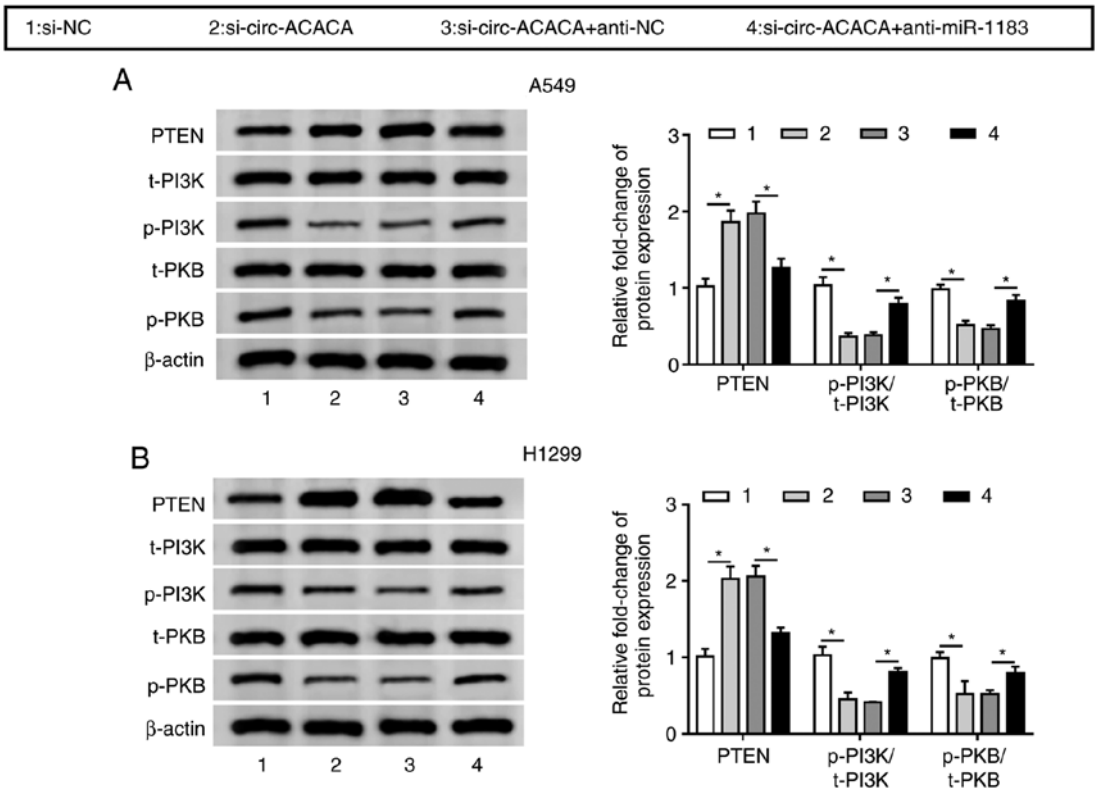

Figure 6. circ-ACACA/miR-1183 axis regulates PI3K/PKB pathway. The protein levels of PTEN, t-PI3K, p-PI3K, t-PKB and p-PKB in (A) A549 and (B) H1299 cells transfected with si-circ-ACACA or si-circ-ACACA + anti-miR-1183, as well as matched controls were checked by western blotting. *P<0.05. circ, circular; si, small interfering; NC, negative control; miR, microRNA; t-PI3K, total-phosphoinositide 3 kinase; p-PKB, phosphorylated-protein kinase B.

Altogether, these results demonstrated that circ-ACACA silencing suppressed proliferation and migration and alleviated the Warburg effect in NSCLC cells.

Downregulation of miR-1183 promotes proliferation and migration and elevates glycolysis rate. To probe the function of miR-1183 in NSCLC, its expression was detected and the data showed that miR-1183 was significantly downregulated in NSCLC tissues and cells compared with normal tissues and cells (Fig. 3A and B). Thereafter, NSCLC cells were transfected with anti-miR-1183 or anti-NC and the results indicated that miR-1183 was significantly decreased in the anti-miR-1183 group (Fig. 3C and D). Next, a CCK-8 assay and transwell assay were performed and the data showed that downregulation of miR-1183 promoted proliferation (Fig. 3E and F) and enhanced the migration ability of NSCLC cells (Fig. 3G and H). In addition, miR-1183 inhibitor increased ECAR in NSCLC cells (Fig. 3I and J). Simultaneously, the protein levels of c-myc, MMP9 and GLUT1 were significantly elevated in the anti-miR-1183 group (Fig. 3K and L). To sum up, these results demonstrated that miR-1183 might act as a tumor suppressor in NSCLC progression *in vitro*.

circ-ACACA targets and negatively regulates miR-1183 in NSCLC. The interaction between circRNAs and miRNAs in cancer is documented in numerous reports (8,9). To probe the relationship between the two, Pearson's correlation coefficient was analyzed and the result indicated that the expression of miR-1183 was negatively associated with circ-ACACA in NSCLC tissues (Fig. 4A). Afterwards, the miR-1183 mimic was introduced to NSCLC cells and the overexpression efficiency was verified (Fig. 4B). By using circular RNA Interactome, circ-ACACA was found to harbor the binding sites of miR-1183 (Fig. 4C). The Dual-luciferase reporter assay showed that miR-1183 significantly diminished the luciferase activity of WT-circ-ACACA in NSCLC cells, rather than MUT-circ-ACACA (Fig. 4D and E). The RIP assay indicated that the relative enrichment of circ-ACACA and miR-1183 was increased in the Anti-Ago2 group compared with the control group (Fig. 4F and G). Simultaneously, RNA pull-down assay showed that circ-ACACA was notably enriched in NSCLC cells transfected with Bio-miR-1183 (Fig. 4H and I). Further study indicated that knockdown of circ-ACACA significantly increased the expression of miR-1183 in NSCLC cells (Fig. 4J and K). All in all, these results demonstrated that miR-1183 was a target of circ-ACACA and negatively modulated by circ-ACACA in NSCLC cells.

Downregulation of miR-1183 reverses circ-ACACA silencing-mediated effects on proliferation, migration and glycolysis rate. To further dissect the impact of the interaction between circ-ACACA and miR-1183 on NSCLC progression, the level of miR-1183 in NSCLC cells infected with si-circ-ACACA or si-circ-ACACA + anti-miR-1183 was first measured, as well as the corresponding controls. The result showed that miR-1183 was significantly upregulated in the si-circ-ACACA group, while its expression was significantly decreased following infection with

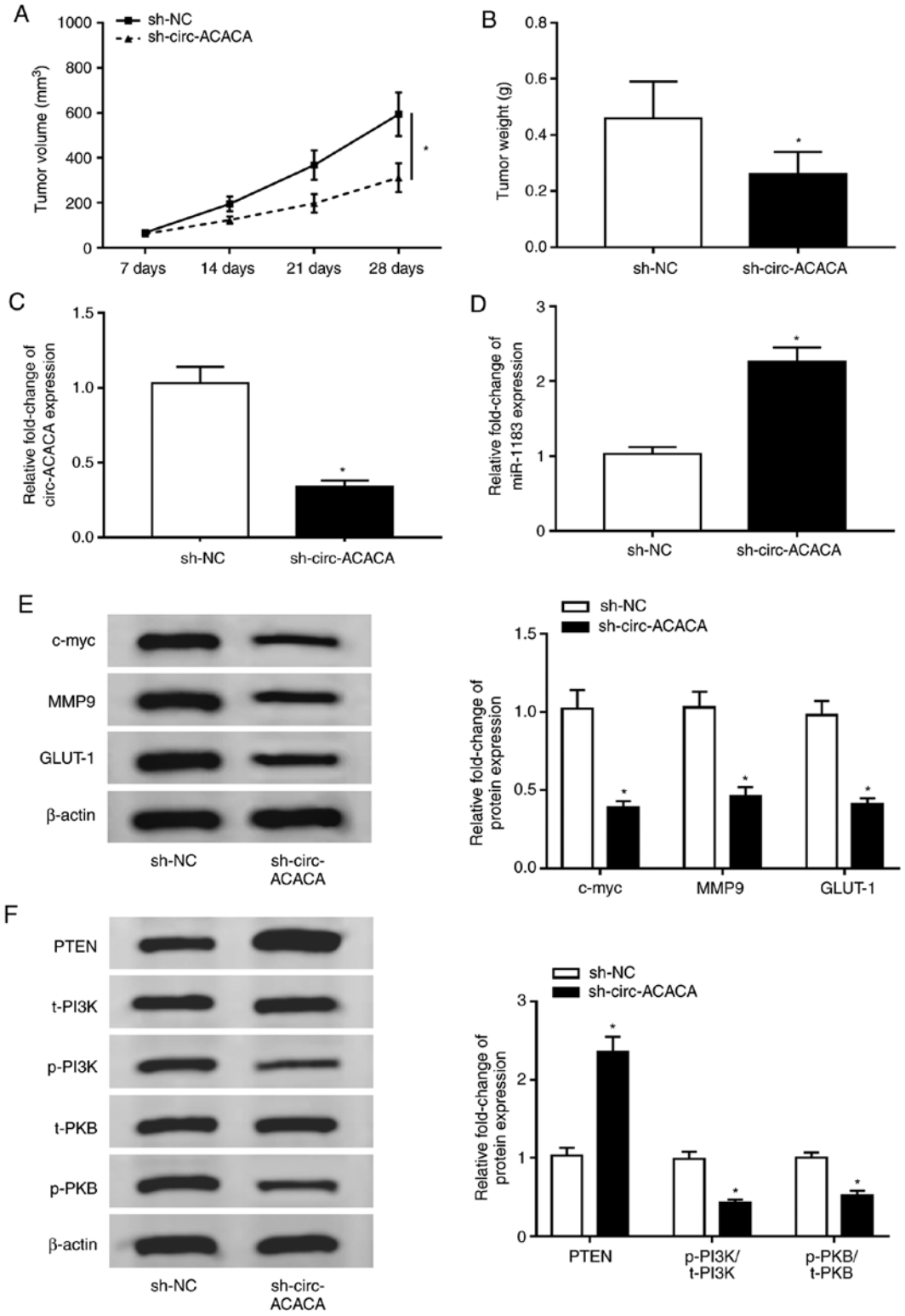

Figure 7. Downregulation of circ-ACACA represses tumor growth. (A) The tumor volume in two groups (n=5) was measured every 7 days. (B) Weight of the resected tumor was examined after the mice were killed. (C) The level of circ-ACACA in NSCLC cells infected with sh-circ-ACACA or sh-NC was measured by RT-qPCR. (D) The level of miR-1183 in NSCLC cells infected with sh-circ-ACACA or sh-NC was measured by RT-qPCR. (E) The protein levels of c-myc, MMP9 and GLUT-1 in tumors were determined by western blotting. (F) The protein levels of PTEN, t-PI3K, p-PI3K, t-PKB and p-PKB in infected NSCLC cells were measured by western blotting. *P<0.05 vs. sh-NC. circ, circular; si, small interfering; NC, negative control; miR, microRNA; t-PI3K, total-phosphoinositide 3 kinase; p-PKB, phosphorylated-protein kinase B; RT-q, reverse transcription-quantitative; NSCLC, non-small cell lung cancer; PTEN, phosphatase and tensin homolog; MMP, matrix metalloproteinases; GLUT, glucose transporter; c-myc, cellular-myelocytomatosis.

anti-miR-1183 (Fig. 5A and B). The CCK-8 assay indicated that downregulation of miR-1183 inverted the circ-ACACA silencing-mediated inhibitory effect on proliferation of NSCLC cells (Fig. 5C and D). The Transwell assay revealed that circ-ACACA silencing-mediated the repressive impact on migration of NSCLC cells and was reversed by the miR-1183

inhibitor (Fig. 5E and F). Similarly, the decreased ECAR in the si-circ-ACACA group was reversed after infection with anti-miR-1183 (Fig. 5G and H). Meanwhile, the declined protein levels of c-myc, MMP9, GLUT-1 in si-circ-ACACA group were reversed by the miR-1183 inhibitor (Fig. 5I and J). From these results, it could be concluded that circ-ACACA mediated the progression of NSCLC by interacting with miR-1183 *in vitro*.

circ-ACACA regulates the PI3K/PKB signaling pathway by interacting with miR-1183 in NSCLC cells. To investigate whether circ-ACACA could affect the PI3K/PKB pathway, the protein levels of PTEN, total PI3K (t-PI3K), p-PI3K, total PKB (t-PKB) and p-PKB in NSCLC cells infected with si-circ-ACACA, si-circ-ACACA + anti-miR-1183 or matched controls were detected. The results indicated that PTEN was significantly upregulated and the levels of p-PI3K/t-PI3K and p-PKB/t-PKB were notably downregulated in the si-circ-ACACA group, whereas the situation was reversed after infection with anti-miR-1183 (Fig. 6A and B). In summary, these results demonstrated that the circ-ACACA/miR-1183 axis regulated the PI3K/PKB pathway in NSCLC.

circ-ACACA silencing inhibits tumor growth in vivo. To verify the function of circ-ACACA in NSCLC cells *in vivo*, the xenograft mouse model was established using A549 cells transfected with sh-circ-ACACA or sh-NC. The data showed that knockdown of circ-ACACA led to an obvious shrink in tumor volume (Fig. 7A) and decline in tumor weight (Fig. 7B). Also, the level of circ-ACACA was significantly decreased in the sh-circ-ACACA group (Fig. 7C), the opposite effect to the expression of miR-1183 (Fig. 7D). In addition, knockdown of circ-ACACA reduced the protein levels of c-myc, MMP9 and GLUT-1 in tumors (Fig. 7E). Similarly, the protein level of PTEN was conspicuously elevated and the protein levels of p-PI3K/t-PI3K and p-PKB/t-PKB were clearly declined in sh-circ-ACACA group (Fig. 7F). Taken together, these results suggested that downregulation of circ-ACACA suppressed NSCLC progression *in vivo*.

Discussion

NSCLC accounts for ~85% of all lung cancers and the five-year survival rate can be very low due to metastasis and drug-resistance (2,3). Therefore, it is essential to find new molecular targets and investigate potential mechanisms. Recently, circRNAs have been verified to regulate the progression of numerous cancers. Liu *et al* (7) found that circular RNA YAP1 inhibited gastric cancer progression via modulating miR-367-5p. Lu *et al* (8) reported that circSLC8A1 suppressed bladder cancer progression via regulating PTEN. Chen *et al* (9) found that circRNA 100146 acted as an oncogene in NSCLC. To explore the function of circ-ACACA in NSCLC, its expression level was checked and it was found that circ-ACACA was upregulated in NSCLC tissues and cells and contributed to poor prognosis. Also, ROC curve analysis indicated that circ-ACACA could be a biomarker for NSCLC. Further analysis showed that downregulation of circ-ACACA hindered proliferation and migration of NSCLC cells. Alteration of energy metabolism, especially abnormal activation of the glycolysis pathway was observed in diverse human cancers (26,27). circRNAs are reported to be involved in the regulation of the Warburg effect in human cancers (28,29). Hence, the level of ECAR were checked in NSCLC cells and it was found that circ-ACACA silencing reduced the glycolysis rate. In addition, the protein levels of c-myc, MMP9 and GLUT-1 also declined in NSCLC cells infected with si-circ-ACACA. Furthermore, *in vivo* experiments showed that knockdown of circ-ACACA repressed tumor growth. All in all, these results suggested that circ-ACACA might function as an oncogene and could be a potential therapeutic target in NSCLC.

Growing evidence has clarified the fact that circRNAs could serve as the sponges of miRNAs to function in numerous cancers (30,31) and the present research showed that circ-ACACA was mainly expressed in the cytoplasm in NSCLC cells. In this study, miR-1183 was forecasted to be a target of circ-ACACA and this interaction was confirmed. A previous report showed that miR-1183 was involved in the regulation of NSCLC progression (18). In this study, the level of miR-1183 was decreased in NSCLC tissues and cells. Moreover, the miR-1183 inhibitor repressed proliferation and migration of NSCLC cells and reduced the glycolysis rate. In-depth studies illustrated that the repressive impact of circ-ACACA silencing-mediated NSCLC progression was reversed by downregulating miR-1183. A previous report indicated that the PI3K/PKB signaling pathway participated in the regulation of NSCLC (32). To investigate whether circ-ACACA affected this pathway, the expression of related proteins in NSCLC cells infected with si-circ-ACACA, si-circ-ACACA + anti-miR-ACACA or corresponding controls was checked. The results indicated circ-ACACA silencing elevated the expression level of PTEN, a major antagonist of PI3K activity and also decreased the levels of p-PI3K/t-PI3K and p-PKB/t-PKB, while downregulation of miR-1183 reversed the effect. These data indicated that the silencing of circ-ACACA inactivating the PI3K/PKB pathway, whereas this effect was abolished by the miR-1183 inhibitor. Taken together, these results suggested that circ-ACACA mediated the proliferation, migration and glycolysis via sponging miR-1183 and the circ-ACACA/miR-1183 axis regulated the PI3K/PKB pathway.

In conclusion, the current research demonstrated that circ-ACACA was upregulated in NSCLC tissues and cells. Also, downregulation of circ-ACACA restrained NSCLC progression via interacting with miR-1183 and inactivating the PI3K/PKB pathway. This novel mechanism may provide a theoretical basis for research into circRNA-directed treatment in NSCLC.

Acknowledgement

Not applicable.

Funding

No funding was received.

Availability of data and materials

The datasets used or analysed during the current study are available from the corresponding author on reasonable request.

Authors' contributions

WW and XY designed the study and drafted the paper. WX and HL performed experiments. MY analyzed the data. All authors were involved in interpreting the results and reviewing the manuscript. All authors read and approved the final manuscript.

Ethics approval and consent to participate

Every patient signed the informed consent and the official approval from the Ethics Committee of Liaocheng People's Hospital was obtained in this study. The animal experiment was approved by the Animal Care and Use Committee of Liaocheng People's Hospital.

Patient consent for publication

Not applicable.

Competing interests

The authors declare that they have no competing interests.

References

1. Liu G, Pei F, Yang F, Li L, Amin AD, Liu S, Buchan JR and Cho WC: Role of autophagy and apoptosis in non-small-cell lung cancer. Int J Mol Sci 18: E367, 2017.
2. Cai J, Fang L, Huang Y, Li R, Xu X, Hu Z, Zhang L, Yang Y, Zhu X, Zhang H, *et al*: Simultaneous overactivation of Wnt/β-catenin and TGFβ signalling by miR-128-3p confers chemoresistance-associated metastasis in NSCLC. Nat Commun 8: 15870, 2017.
3. Cheng H and Perez-Soler R: Leptomeningeal metastases in non-small-cell lung cancer. Lancet Oncol 19: e43-e55, 2018.
4. Kristensen LS, Andersen MS, Stagsted LVW, Ebbesen KK, Hansen TB and Kjems J: The biogenesis, biology and characterization of circular RNAs. Nat Rev Genet 20: 675-691, 2019.
5. Jeck WR, Sorrentino JA, Wang K, Slevin MK, Burd CE, Liu J, Marzluff WF and Sharpless NE: Circular RNAs are abundant, conserved, and associated with ALU repeats. RNA 19: 141-157, 2013.
6. Ju HQ, Zhao Q, Wang F, Lan P, Wang Z, Zuo ZX, Wu QN, Fan XJ, Mo HY, Chen L, *et al*: A circRNA signature predicts postoperative recurrence in stage II/III colon cancer. EMBO Mol Med 11: e10168, 2019.
7. Liu H, Liu Y, Bian Z, Zhang J, Zhang R, Chen X, Huang Y, Wang Y and Zhu J: Circular RNA YAP1 inhibits the proliferation and invasion of gastric cancer cells by regulating the miR-367-5p/p27 kip1 axis. Mol Cancer 17: 151, 2018.
8. Lu Q, Liu T, Feng H, Yang R, Zhao X, Chen W, Jiang B, Qin H, Guo X, Liu M, *et al*: Circular RNA circSLC8A1 acts as a sponge of miR-130b/miR-494 in suppressing bladder cancer progression via regulating PTEN. Mol Cancer 18: 111, 2019.
9. Chen L, Nan A, Zhang N, Jia Y, Li X, Ling Y, Dai J, Zhang S, Yang Q, Yi Y and Jiang Y: Circular RNA 100146 functions as an oncogene through direct binding to miR-361-3p and miR-615-5p in non-small cell lung cancer. Mol Cancer 18: 13, 2019.
10. Wu K, Liao X, Gong Y, He J, Zhou JK, Tan S, Pu W, Huang C, Wei YQ and Peng Y: Circular RNA F-circSR derived from SLC34A2-ROS1 fusion gene promotes cell migration in non-small cell lung cancer. Mol Cancer 18: 98, 2019.
11. Yang L, Wang J, Fan Y, Yu K, Jiao B and Su X: Hsa_circ_0046264 up-regulated BRCA2 to suppress lung cancer through targeting hsa-miR-1245. Respir Res 19: 115, 2018.
12. Gebert LFR and MacRae IJ: Regulation of microRNA function in animals. Nat Rev Mol Cell Biol 20: 21-37, 2019.
13. Peng Y and Croce CM: The role of MicroRNAs in human cancer. Signal Transduct Target Ther 1: 15004, 2016.
14. Tan W, Liu B, Qu S, Liang G, Luo W and Gong C: MicroRNAs and cancer: Key paradigms in molecular therapy. Oncol Lett 15: 2735-2742, 2018.
15. Antônio LGL, Freitas-Lima P, Pereira-da-Silva G, Assirati JA Jr, Matias CM, Cirino MLA, Tirapelli LF, Velasco TR, Sakamoto AC, Carlotti CG Jr and Tirapelli DPDC: Expression of MicroRNAs miR-145, miR-181c, miR-199a and miR-1183 in the blood and hippocampus of patients with mesial temporal lobe epilepsy. J Mol Neurosci 69: 580-587, 2019.
16. Cheng X, Ander BP, Jickling GC, Zhan X, Hull H, Sharp FR and Stamova B: MicroRNA and their target mRNAs change expression in whole blood of patients after intracerebral hemorrhage. J Cereb Blood Flow Metab: April 9, 2019 (Epub ahead of print).
17. Prahm KP, Høgdall C, Karlsen MA, Christensen IJ, Novotny GW and Høgdall E: Identification and validation of potential prognostic and predictive miRNAs of epithelial ovarian cancer. PLoS One 13: e0207319, 2018.
18. Zhou Y, Zheng X, Xu B, Chen L, Wang Q, Deng H and Jiang J: Circular RNA hsa_circ_0004015 regulates the proliferation, invasion, and TKI drug resistance of non-small cell lung cancer by miR-1183/PDPK1 signaling pathway. Biochem Biophys Res Commun 508: 527-535, 2019.
19. Nicholson KM and Anderson NG: The protein kinase B/Akt signalling pathway in human malignancy. Cell Signal 14: 381-395, 2002.
20. Mahajan K and Mahajan NP: PI3K-independent AKT activation in cancers: A treasure trove for novel therapeutics. J Cell Physiol 227: 3178-3184, 2012.
21. Dong P, Konno Y, Watari H, Hosaka M, Noguchi M and Sakuragi N: The impact of microRNA-mediated PI3K/AKT signaling on epithelial-mesenchymal transition and cancer stemness in endometrial cancer. J Transl Med 12: 231, 2014.
22. Chen K, Abuduwufuer A, Zhang H, Luo L, Suotesiyali M and Zou Y: SNHG7 mediates cisplatin-resistance in non-small cell lung cancer by activating PI3K/AKT pathway. Eur Rev Med Pharmacol Sci 23: 6935-6943, 2019.
23. Livak KJ and Schmittgen TD: Analysis of relative gene expression data using real-time quantitative PCR and the 2(-Delta Delta C(T)) method. Methods 25: 402-408, 2001.
24. Dudekula DB, Panda AC, Grammatikakis I, De S, Abdelmohsen K and Gorospe M: CircInteractome: A web tool for exploring circular RNAs and their interacting proteins and microRNAs. RNA Biol 13: 34-42, 2016.
25. Zhang X, Zhuang J, Liu L, He Z, Liu C, Ma X, Li J, Ding X and Sun C: Integrative transcriptome data mining for identification of core lncRNAs in breast cancer. PeerJ 7: e7821, 2019.
26. Hua Q, Jin M, Mi B, Xu F, Li T, Zhao L, Liu J and Huang G: LINC01123, a c-Myc-activated long non-coding RNA, promotes proliferation and aerobic glycolysis of non-small cell lung cancer through miR-199a-5p/c-Myc axis. J Hematol Oncol 12: 91, 2019.
27. Yang J, Ren B, Yang G, Wang H, Chen G, You L, Zhang T and Zhao Y: The enhancement of glycolysis regulates pancreatic cancer metastasis. Cell Mol Life Sci 77: 305-321, 2020.
28. Li Q, Pan X, Zhu D, Deng Z, Jiang R and Wang X: Circular RNA MAT2B promotes glycolysis and malignancy of hepatocellular carcinoma through the miR-338-3p/PKM2 axis under hypoxic stress. Hepatology 70: 1298-1316, 2019.
29. Zhang X, Wang S, Wang H, Cao J, Huang X, Chen Z, Xu P, Sun G, Xu J, Lv J and Xu Z: Circular RNA circNRIP1 acts as a microRNA-149-5p sponge to promote gastric cancer progression via the AKT1/mTOR pathway. Mol Cancer 18: 20, 2019.
30. Han D, Li J, Wang H, Su X, Hou J, Gu Y, Qian C, Lin Y, Liu X, Huang M, *et al*: Circular RNA circMTO1 acts as the sponge of microRNA-9 to suppress hepatocellular carcinoma progression. Hepatology 66: 1151-1164, 2017.
31. Yang J, Cong X, Ren M, Sun H, Liu T, Chen G, Wang Q, Li Z, Yu S and Yang Q: Circular RNA hsa_circRNA_0007334 is predicted to promote MMP7 and COL1A1 expression by functioning as a miRNA sponge in pancreatic ductal adenocarcinoma. J Oncol 2019: 7630894, 2019.
32. Pérez-Ramírez C, Cañadas-Garre M, Molina M, Faus-Dáder MJ and Calleja-Hernández M: PTEN and PI3K/AKT in non-small-cell lung cancer. Pharmacogenomics 16: 1843-1862, 2015.